doi.org/10.15392/2319-0612.2025.2765
Braz. J. Radiat. Sci., Rio de Janeiro
2025, 13(1) | 01-22 | e2765
Editor: Prof. Dr. Bernardo Maranhão Dantas
Submitted: 2024-09-03
Accepted: 2024-12-16

Considering the Figure of Merit as a parameter of optimization in Mammography: a case study of the performance in a CR and a DR system

Contassot[a*], R. X.; Catusso[b], L.; Silva[c], I. R. V.; Garrafiel[d], F. N.; Azevedo[e], D. S.; Ferreira[f], C. C.; Estácio[f], M. C. A. E.; Santos[f], F. A.; Valença[c], J. V. B.

[a] Hospital de Clínicas de Porto Alegre, 90035-903, Porto Alegre, Rio Grande do Sul, Brasil.
[b] Universidade Federal de Uberlândia, 38408-100, Uberlândia, Minas Gerais, Brasil.
[c] Universidade Federal de Ciências da Saúde de Porto Alegre, 90050-170, Porto Alegre, Rio Grande do Sul, Brasil.
[d] Hospital São Lucas da PUCRS, 90610-001, Porto Alegre, Rio Grande do Sul, Brasil.
[e] Centro de Desenvolvimento da Tecnologia Nuclear, 31270-901, Belo Horizonte, Minas Gerais, Brasil.
[f] Hospital Universitário da UFS, 49060-108, Aracaju, Sergipe, Brasil.

*Correspondence: raissacontassot@gmail.com

Abstract: Mammography is an important examination for the early detection of breast cancer, and its use requires radiation protection considerations to ensure the lowest possible risk to the patient. The Figure of Merit (FOM) is a commonly used tool to quantify the relation between image quality and radiation dose. Higher FOM values suggest the most appropriate set of radiographic parameters to use in the examination. The objective of this study was to use the FOM as a metric for evaluating the optimization of two different clinical practices, one using a computed radiography (CR) system and the other using a digital radiography (DR) system. For both systems, three PMMA thicknesses were used (2, 4 and 7 cm), and acquisitions were performed at four voltage values commonly applied in clinical routines. Manual and automatic exposure modes were used for both systems. The CR system used Mo/Mo and Mo/Rh target-filter combinations, while the DR system used W/Rh and W/Ag. The image quality parameter used was the Contrast-to-Noise Ratio (CNR), and the considered dosimetric quantity was the Mean Glandular Dose (MGD). The FOMs presented relevant dependence on voltage and PMMA thicknesses, as well as variations with the different target-filter combinations. For both systems, when using 2 cm of PMMA, the FOM results were higher in the automatic acquisition mode. For 4 and 7 cm of PMMA, however, manual parameter adjustments became more relevant. These results reinforce the value of FOM as an important parameter in determining the most suitable acquisition settings for each analyzed equipment.

Keywords: figure of merit, optimization, image quality, mammography.

doi.org/10.15392/2319-0612.2025.2765
Braz. J. Radiat. Sci., Rio de Janeiro
2025, 13(1) | 01-22 | e2765
Editor: Prof. Dr. Bernardo Maranhão Dantas
Submitted: 2024-09-03
Accepted: 2024-12-16

Considerando a Figura de Mérito como parâmetro de otimização em Mamografia: estudo de caso da performance em sistemas CR e DR

Resumo: A mamografia é um exame importante para a detecção precoce do câncer de mama, e o seu uso requer considerações sobre radioproteção a fim de garantir o menor risco ao paciente. A Figura de Mérito (FOM) é uma ferramenta utilizada para quantificar a relação entre qualidade de imagem e dose de radiação. Valores mais altos de FOM sugerem o uso do conjunto de parâmetros radiográficos mais adequado para o exame. O objetivo deste trabalho é considerar a FOM como uma métrica para avaliar a otimização de duas diferentes práticas clínicas, uma com o uso de Sistema CR e outra com o Sistema DR. Para ambos os sistemas, três espessuras de PMMA foram utilizadas (2, 4 e 7 cm), e as aquisições foram realizadas para quatro valores de tensão comumente aplicados na rotina clínica. Foram utilizados os modos manual e automático. O sistema CR envolveu uso de Mo/Mo e Mo/Rh como combinações alvo-filtro, enquanto o sistema DR utilizou W/Rh e W/Ag. O parâmetro de qualidade de imagem usado foi a razão contraste-ruído (CNR), e a grandeza dosimétrica considerada foi a dose glandular média (MGD). Os valores de FOM obtidos apresentaram dependência relevante com as tensões e espessuras de PMMA, bem como variações com as diferentes combinações alvo-filtro aplicadas. Para ambos os sistemas, utilizando 2 cm de PMMA, os resultados de FOM foram maiores ao utilizar o modo automático de aquisição. Para 4 e 7 cm de PMMA, entretanto, ajustes manuais dos parâmetros tornaram-se mais relevantes. Estes resultados reforçam o valor de FOM como um importante parâmetro na determinação do melhor conjunto de parâmetros de aquisição para cada equipamento analisado.

Palavras-chave: figura de mérito, otimização, qualidade da imagem, mamografia.

1. INTRODUCTION

Breast cancer is the type of cancer that most affects women in the world (excluding non-melanoma skin cancer) [1]. In 2020, breast cancer has represented more than a quarter of new cases diagnosed in women worldwide [1]. Each year in the United States, breast cancer represents 1 in every 3 new female cancer diagnoses [2]. For the period 2023-2025, Brazilian National Cancer Institute (INCA) has estimated 73.610 new cases of breast cancer in Brazil [3]. The early diagnosis provides a reduction in mortality and morbidity rates [4], and mammography is an essential examination in this process.

Since its initial conceptualization, mammography has considerably evolved [5, 6, 7]. The screen-film modality has been replaced to computed (CR) and digital radiology (DR) due to improvements in aspects such as the contrast resolution, the obtaining and the processing of the images [7, 8]. Regardless of the used system, it is essential to consider radiation protection aspects during the examination.

The glandular tissue of the breast is most sensitive to ionizing radiation [9, 10]. In these terms, the Mean Glandular Dose (MGD) comes up as a quantity that estimates the absorbed dose in this tissue [9, 10, 11], making it possible to specifically evaluate the breast dose. The Contrast-to-Noise Ratio (CNR) is a metric related to the image quality in which the signal level relative to the noise in an image is considered, being applicable when the analyzed object, such as a relatively small Aluminum foil, produces a homogeneous signal [12].

It is important to establish a balance between image quality and dose in mammography [13, 14]. The Figure of Merit (FOM) is a metric that relates these two parameters, correlating, in many studies, the CNR and the MGD [10, 15, 16]. The relation is given by the square of the CNR divided by the MGD. This value aims to quantify the optimization of a mammography system [17], presenting itself as a single number [17, 18].

OPEN ACCESS

In these terms, some authors have shown that the higher the FOM, the better tend to be the performance of the system [17, 18, 19]. Obtaining and discussing the FOM value for the different set of parameters used in clinical practice can be considered a relevant analysis, so that it is possible to acquire an indication of optimization in terms of image quality and radiation dose, respecting radiation protection concepts.

Different parameters have been studied with regards to their influence on the FOM, such as the peak voltage (kVp), the current-time product (mAs), the thickness of the breast, and the target-filter combination [9, 11, 18]. Nunes et al. (2020) analyzed direct digital mammography systems and concluded that among the studied target-filter combinations (Mo/Mo, Mo/Rh and W/Rh), the use of W/Rh offered the best trade-off between MGD and image quality related parameters [13]. Several studies demonstrated a decrease in the FOM values as the thicknesses of the analyzed phantoms are incremented [9, 10, 20]. With regards to the kVp, even though several studies have found a considerable relation with the FOM [9, 16, 19, 21], Morais et al. (2021) and Perez et al. (2017) obtained results in the opposite direction [20, 22].

Various protocols that approach dosimetry and radiation protection concerning diagnostic radiology have been published worldwide, such as the European Guidelines for Quality Assurance in Breast Cancer Screening and Diagnosis and the TRS 457 [23, 24]. In Brazil, the CNEN NN 3.01 regulation, in accordance with ICRP publication n° 103 [25], establishes three fundamental principles for radiation protection, which are justification, limitation of individual dose, and optimization. The principle of optimization ensures that protection is designed to keep doses, the number of people exposed, and the number of exposures as low as reasonably achievable (ALARA principle) [26]. The mammography should follow this principle to guarantee that the examination exposes the patient to the lowest risk of inducing breast cancer [9, 10, 16], maintaining the diagnostic effectiveness, which reinforces the importance of analyzing the Figure of Merit [13, 14, 20].

OPEN ACCESS

In this context, it is important to understand radiation protection alongside the reasons for, and the consequences of, optimizing the radiographic system. This includes both the necessity of optimization and the natural outcome of applying the ALARA principle.

The main goal of this study was to evaluate the clinical protocols used in mammography by analyzing the performance of a CR and a DR system through the Figure of Merit. Various parameters, such as thickness, kVp, and target/filter combinations, were varied to assess the trends of the metric in each case.

2. MATERIALS AND METHODS

2.1 Mammographic Image Acquisitions

2.1.1 CR System

The acquisitions related to the CR system were made in a hospital to be called Hospital A from now on. A Graph Mammo AF, developed by Philips, was the mammography system used in the analysis. The equipment presented a Molybdenum anode and two different filter options (Molybdenum and Rhodium), reaching a maximum peak voltage of 35 kV and a theoretical maximum current-time product of 600 mAs. Imaging plate processing was performed in a digitizer from AGFA HealthCare, model CR30-Xm.

Three different thicknesses of Polymethyl Methacrylate (PMMA) were used for the exposures: 2, 4, and 7 cm. An Aluminum foil (1 cm x 1 cm) of 0.2 mm thickness was placed on top of the PMMA plates. Considering its center, a distance was kept from the chest wall and the left side from the operator perspective of 3 and 3.5 cm, respectively. The large focal spot and the flat field mode were selected with a full open field (18 x 24 cm^2). The two possible target-filter combinations were used in the evaluations (Mo/Mo and Mo/Rh). Four values (24, 26, 28, and 30 kV) were selected for the peak voltage and the current was fixed by the

OPEN ACCESS

equipment at 70 mA for all measurements in the manual mode of acquisition, following the method commonly used in the clinical practice of this institution. The current-time product was adjusted automatically. Using the Automatic Exposure Control (AEC), two images of each thickness were obtained, one for each target-filter combination previously used.

In order to measure the Entrance Surface Air Kerma (ESAK), needed for the estimation of the MGD, a parametric solid state multidetector from RTI, model Black Piranha, with a calibration certificate LABPROSAUD-C290-19, was used. This detector was positioned 3 cm from the chest wall. In order to obtain the values of the kerma and the half-value layer, the exposures were performed for each set of parameters used in both modes of acquisition (manual and automatic). These results were corrected following conversion factors. The MGD was calculated using Equation 1 [27], where K is the corrected kerma, g corresponds to the glandularity of the breast (50%), c corresponds to the breast composition and s is related to the X-ray spectrum.

$$MGD = K \cdot g \cdot c \cdot s \tag{1}$$

A linear interpolation was used to obtain the values of g and c factors, based on the ones listed by Dance et al. (2000) [27]. The s factor was also obtained from this reference.

2.1.2 DR System

The used DR system, located in Hospital B, was a Selenia Dimensions, from Hologic, which presents a Tungsten anode, along with Rhodium, Aluminum, Silver, Copper and Lead as possible filters. The peak voltage varies between 20 and 49 kV and the current-time product varies in a range from 3 to 500 mAs.

The thicknesses of the PMMA plates, the field size and the peak voltages were the same employed in the CR system analysis. The use of these values for PMMA thicknesses represents a form to simulate three general sizes of breast - small, medium, and large. The use of the kVp range relies on the fact that these are the values most applied in clinical practice

OPEN ACCESS

for both institutions. The contrast object was also an Aluminum foil (2 cm x 2 cm) of 0.2 mm thickness, and the positioning was the same employed on the CR system. W/Rh and W/Ag were the chosen target-filter combinations in the analysis, as they are the combinations used in the hospital routine and are quoted to offer the best trade-off between image quality and dose in digital systems [13, 19]. Willing to simulate the clinical practice, the automatic mode of acquisition was used, with the current and the current time product being adjusted automatically. Two types of AEC were used for the acquisitions, one that adjusts automatically the peak voltage (Auto kV) and the other one that adjusts the target-filter combination (Auto Filter), for each of the thicknesses used in the manual mode. The system provided the MGD automatically for each exposure, which was used in the FOM analysis.

2.2 Image Analysis

The raw images were analyzed using the free software *ImageJ* [28]. A 5 x 5 mm^2 Region of Interest (ROI) was placed in the contrast object representation and another ROI of the same size was positioned 20 mm on top of the first one to obtain the background signal. The size of the ROI was defined based on previous studies [9, 15, 16, 18, 22], so that the discussion can be applied comparing similar methodologies. The mean and the standard deviation for each ROI were used to calculate the CNR. Figure 1 shows an example of the ROIs defined in the software, where ROI 1 corresponds to the signal of the contrast object, and ROI 2 corresponds to the background.

Figure 1: Representation of the ROIs defined on *ImageJ*.

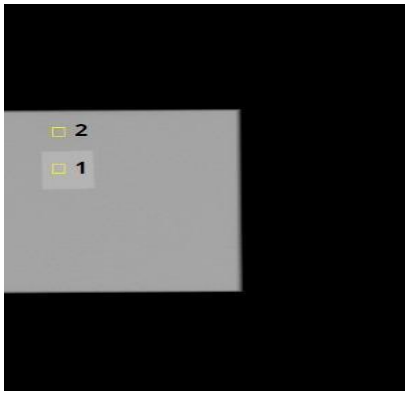

OPEN ACCESS
CC BY

2.3 Obtaining the CNR and the FOM

The CNR is a metric that describes the signal related to the noise of an image, being applied to the cases where the medium gray scale in the ROI represents the entire object [12]. It can be calculated by two usual forms, described by Equations 2 and 3. Equation 2 has been used in publications that approach the FOM [15, 20, 29] and does not consider the standard deviation related to the signal. Equation 3 is defined by the European Protocol [23] and it is commonly applied to digital systems [9]. The difference between these two equations is in the consideration of the standard deviation related to the background, which adds to Equation 3 one more metric for the image quality evaluation. The mean and the standard deviation for the signal are given by $\underline{X_s}$ and σ_s, respectively. For the background, the mean is given by $\underline{X_{bg}}$ and the standard deviation is σ_{bg}.

$$CNR1 = \frac{|\underline{X_s} - \underline{X_{bg}}|}{\sigma_{bg}} \tag{2}$$

$$CNR2 = \frac{|\underline{X_s} - \underline{X_{bg}}|}{\sqrt{\frac{\sigma_s^2 + \sigma_{bg}^2}{2}}} \tag{3}$$

The FOM is a parameter that contributes to quantifying the optimization of a mammography system and there are several ways to calculate this metric [17]. One of the most explored methods for calculating the FOM is to relate the CNR to the MGD, being described by Equation 4 [14, 15, 16, 17, 18, 20, 22, 30]. In this study, the FOM was measured using both values for CNR, obtained by the application of Equations 2 and 3, being called FOM1 and FOM2, respectively.

$$FOM = \frac{CNR^2}{MGD} \tag{4}$$

OPEN ACCESS

3. RESULTS AND DISCUSSIONS

3.1 CR System

Table 1 shows the parameters used for the analysis of the FOM. It is possible to see that for a specific measure configuration in the manual mode of acquisition (7 cm of PMMA, 30 kVp, Mo/Mo) and in a specific use of AEC (4 cm of PMMA, 27 kVp, Mo/Mo), the MGD is above the acceptable level established by international and brazilian rules concerning mammography [31, 32]. However, considering the 5% uncertainty related to the MGD (value connected to the Black Piranha specification), these results may be on the acceptable level. The performance of examinations using a set of technical parameters that are not suitable for obtaining images with minimal diagnostic quality and/or adequate dose levels are not feasible, which becomes evident, for example, in non-compliance with the regulated dose levels. This reinforces the importance of medical physicists in the institutions, in order to optimize the practices considering radiation protection aspects.

Table 1 : Parameters used in the analysis for the CR system.

PMMA Thicknesses (cm)	Peak Voltage (kVp)	Target-Filter	mAs	Achievable MGD* (mGy)	Acceptable MGD* (mGy)	MGD (mGy)	CNR1	CNR2
2	24	Mo/Mo	32	0.6	1.0	0.620 ± 0.031	12.981	12.241
		Mo/Rh	14			0.258 ± 0.013	8.767	8.263
	26	Mo/Mo	22			0.658 ± 0.033	12.616	12.221
		Mo/Rh	10			0.292 ± 0.015	8.574	8.259
	28	Mo/Mo	15			0.691 ± 0.034	12.281	11.800
		Mo/Rh	10			0.468 ± 0.023	9.477	9.009
	30	Mo/Mo	11			0.672 ± 0.033	12.248	11.668
		Mo/Rh	10			0.621 ± 0.031	11.806	11.244
	23 (AEC)	Mo/Mo	46			0.650 ± 0.032	13.837	13.063
	23 (AEC)	Mo/Rh	31			0.430 ± 0.021	10.732	10.150
4	24	Mo/Mo	151	1.6	2.0	1.685 ± 0.084	10.231	9.743
		Mo/Rh	74			0.857 ± 0.043	6.945	6.662

OPEN ACCESS

PMMA Thicknesses (cm)	Peak Voltage (kVp)	Target-Filter	mAs	Achievable MGD* (mGy)	Acceptable MGD* (mGy)	MGD (mGy)	CNR1	CNR2
	26	Mo/Mo	99			1.729 ± 0.086	10.174	9.819
		Mo/Rh	52			0.972 ± 0.048	7.509	7.217
	28	Mo/Mo	78			1.964 ± 0.098	10.151	9.898
		Mo/Rh	39			1.118 ± 0.056	7.580	7.284
	30	Mo/Mo	46			1.731 ± 0.086	9.324	8.909
		Mo/Rh	26			1.094 ± 0.055	7.328	7.053
	27 (AEC)	Mo/Mo	97			2.084 ± 0.100	10.374	10.009
	25 (AEC)	Mo/Rh	66			1.069 ± 0.053	7.229	6.828
7	24	Mo/Mo	299	5.1	6.5	2.155 ± 0.100	1.019	0.981
		Mo/Rh	299			2.233 ± 0.110	2.290	2.184
	26	Mo/Mo	299			3.508 ± 0.170	2.416	2.338
		Mo/Rh	290			3.662 ± 0.180	3.136	2.917
	28	Mo/Mo	299			5.114 ± 0.250	3.489	3.349
		Mo/Rh	259			4.870 ± 0.240	4.259	3.938
	30	Mo/Mo	267			6.612 ± 0.330	3.461	3.281
		Mo/Rh	201			5.343 ± 0.260	4.239	3.947
	30 (AEC)	Mo/Mo	268			6.205 ± 0.310	3.627	3.470
	30 (AEC)	Mo/Rh	216			5.583 ± 0.280	4.254	4.136

*Level established by [31, 32].

Figures 2, 3, and 4 show the behavior of FOM1 and FOM2 for each of the analyzed PMMA thicknesses. The uncertainty related to the CNR was, in a first approximation, fixed at 0.1 with the aim of finding, via uncertainty propagation, the value associated with the FOM also considering a value for the CNR. This value was used considering the intrinsic characteristics of obtaining CNR values with equations 2 and 3, as well as the fact that a single exposure was performed for each parameter configuration used. For the same target-filter combination, both FOMs present a similar tendency for the curves. In most cases, FOM1 was higher than FOM2 (approximately 9%, considering the mean between the

OPEN ACCESS

differences for each exposure). Considering the mean values, for 2 cm of PMMA, it is possible to see a decay on the FOM up to 28 kVp and the higher value in 24 kVp for both target-filter combinations. For 4 cm, both FOMs for Mo/Mo are higher in 24 kVp, and for Mo/Rh are higher in 26 kVp. For 7 cm, the highest FOM values were found using 28 kVp for both Mo/Mo and Mo/Rh.

Although previous studies found that Mo/Mo is the best choice for thinner breasts [20], Perez et al. (2017), for example, found that the highest FOM was always obtained using Mo/Rh or Rh/Rh, but never using Mo/Mo [22]. Considering the analyzed range of peak voltages used in this study, for 2 cm of PMMA the use of both Mo/Mo (AEC) and Mo/Rh (manual mode) may achieve similar values for the FOM. For 4 and 7 cm, the best combinations, with regards to the optimum relation between CNR and MGD, are Mo/Mo and Mo/Rh, respectively.

The AEC values presented on the graphs were obtained using FOM1, since the results were also higher when compared to FOM2. For both anode-filter combinations, the AEC selected 23 kVp for the beam production when 2 cm of PMMA was used. Using the Mo/Mo combination, the AEC provided the highest FOM value, whereas for the Mo/Rh the manual use of 24 kVp provided the highest value. For 4 cm of PMMA, the highest FOM of the AEC was obtained using Mo/Mo for 27 kVp. However, the MGD value exceeded the established acceptable level, which makes this set of parameters unfeasible to be used in the practice. The optimal choice for this breast thickness is given by the use of the manual mode, since the highest FOM were obtained in 24 kVp (Mo/Mo). For 7 cm of PMMA, both FOMs of AEC were obtained for 30 kVp. The use of Mo/Rh has provided the highest values for both modes of acquisition, but in the manual mode, the spectrum generated by 28 kVp has presented itself as the best choice. These results highlight the importance of the optimization analysis, which may objectively contribute to the discussion about the use of the equipment in different situations.

OPEN ACCESS

The increase in the thickness of PMMA has caused a decrease in the values of the FOMs, a fact that goes along with the findings of previous studies [10, 16, 20, 33, 34]. The explanation of this behavior is related to the higher influence of the scattered radiation in the image acquisitions.

Figure 2: Relation between FOM and Peak Voltage for 2 cm of PMMA in the analyzed CR system.

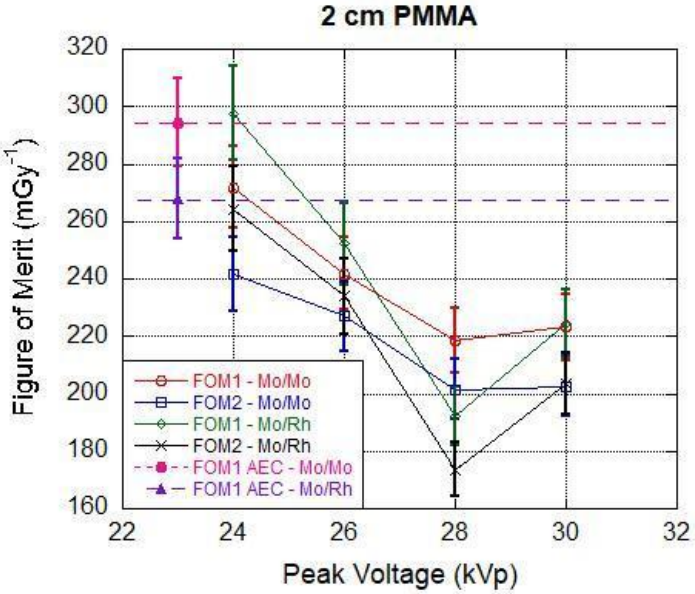

Figure 3: Relation between FOM and Peak Voltage for 4 cm of PMMA in the analyzed CR system.

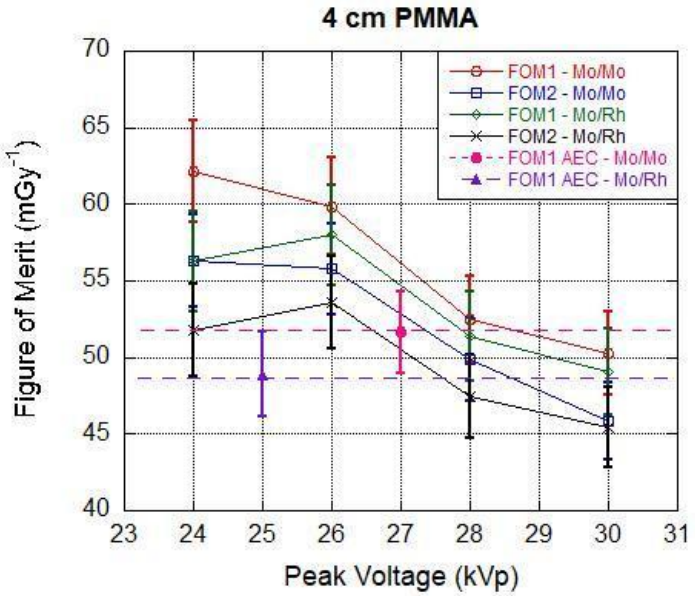

OPEN ACCESS
CC BY

Figure 4: Relation between FOM and Peak Voltage for 7 cm of PMMA in the analyzed CR system.

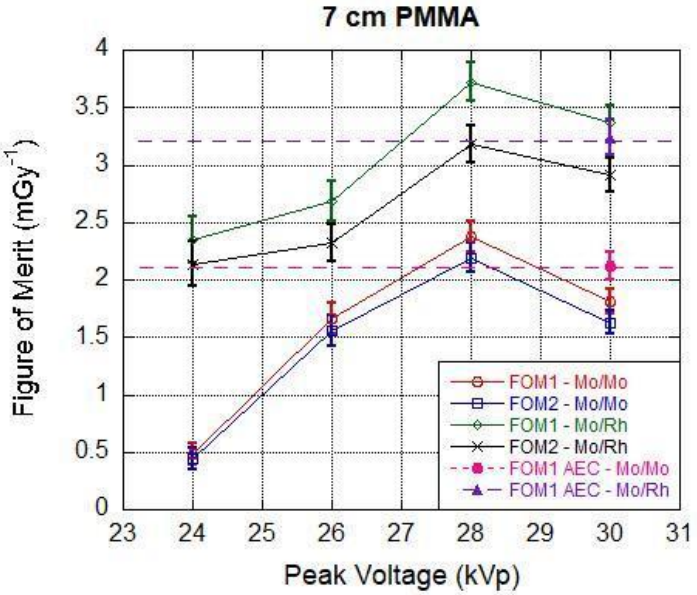

3.2 DR System

Table 2 shows the parameters used to analyze the FOM for the DR system. The equipment did not allow the acquisition for 2 cm of PMMA using W/Ag for 30 kVp, due to the fact that the required mAs was considered too low. This situation was also found for 7 cm of PMMA using W/Rh for 24 and 26 kVp and using W/Ag for 24 kVp, but in these cases, the indication in the equipment was that the required mAs was too high. Considering the international and brazilian established limits [31, 32], there is no MGD value above the acceptable level. Moreover, all values found for MGD using 4 and 7 cm of PMMA are within the achievable level.

Table 2 : Parameters used in the analysis for the DR system.

PMMA Thicknesses (cm)	Peak Voltage (kVp)	Target-Filter	mAs	Achievable MGD* (mGy)	Acceptable MGD* (mGy)	MGD (mGy)	CNR1	CNR2
2	24	W/Rh	57	0.6	1.0	0.64	9.115	9.452
		W/Ag	49			0.65	8.227	8.513
	26	W/Rh	43			0.66	8.997	9.329
		W/Ag	29			0.55	7.259	7.522

OPEN ACCESS
CC BY

PMMA Thicknesses (cm)	Peak Voltage (kVp)	Target-Filter	mAs	Achievable MGD* (mGy)	Acceptable MGD* (mGy)	MGD (mGy)	CNR1	CNR2
	28	W/Rh	34			0.66	8.624	8.931
		W/Ag	21			0.53	6.914	7.091
	30	W/Rh	25			0.61	7.983	8.245
		W/Ag	-			-	-	-
	25 (Auto kV)	W/Rh	47			0.64	9.299	9.622
	25 (Auto Filter)	W/Rh	46			0.62	9.045	9.529
4	24	W/Rh	148	1.6	2.0	1.08	7.161	7.395
		W/Ag	130			1.10	6.710	6.926
	26	W/Rh	105			1.05	7.215	7.520
		W/Ag	71			0.90	6.073	6.338
	28	W/Rh	77			1.00	6.877	7.181
		W/Ag	49			0.85	5.875	6.054
	30	W/Rh	59			0.96	6.376	6.623
		W/Ag	38			0.80	5.733	5.898
	28 (Auto kV)	W/Rh	92			1.16	7.367	7.591
	25 (Auto Filter)	W/Rh	92			1.22	7.470	7.775
7	24	W/Rh	-	5.1	6.5	-	-	-
		W/Ag	-			-	-	-
	26	W/Rh	-			-	-	-
		W/Ag	282			2.32	5.171	5.327
	28	W/Rh	356			3.06	5.743	5.902
		W/Ag	194			2.18	5.160	5.274
	30	W/Rh	235			2.54	5.123	5.286
		W/Ag	143			2.07	4.953	5.086
	34 (Auto kV)	W/Rh	230			3.57	4.564	4.611
	30 (Auto Filter)	W/Ag	294			4.33	6.629	6.873

*Level established by [31, 32].

Figures 5, 6, and 7 show the behavior of the FOMs for 2, 4 and 7 cm of PMMA, respectively. The uncertainty related to the CNR was also fixed at 0.1, and at 0.01 for the MGD. Considering the same anode-filter combination, FOM1 and FOM2 generated similar

OPEN ACCESS

tendencies for the curves. In most cases, FOM2 was higher than FOM1 (almost 6%, considering the mean between the differences for each exposure). The manual mode did not provide the best choice for 2 cm of PMMA and the highest value for the FOM corresponds to the use of W/Rh at 24 kVp. For 4 cm, the highest value was found using W/Rh at 26 kVp. For 7 cm, the use of W/Ag at 28 kVp has presented itself as the best choice.

For the studied range of peak voltages, the use of W/Rh was the most suitable choice for 2 and 4 cm of PMMA. For 7 cm, the most appropriate combination was W/Ag. Previous studies reported that the use of W/Rh provides advantages in terms of radiation protection, dose and image quality [13, 19], in addition to the fact that W/Ag was indicated for breast thicknesses greater than 6 cm [19].

The values obtained using the AEC modes of acquisition that are presented on the graphs correspond to FOM2, because the results were also higher than the ones for FOM1. For 2 and 4 cm of PMMA, the automatic modes selected W/Rh for 25 and 28 kVp, respectively. For 7 cm, the auto kV mode selected W/Rh for 34 kVp and the auto filter mode selected W/Ag for 30 kVp. The use of both auto kV or auto filter represent a suitable choice for thinner breasts. On the other hand, for medium and thicker breasts, the use of the manual set of parameters has provided higher values for the FOM.

Figure 5: Relation between FOM and Peak Voltage for 2 cm of PMMA in the analyzed DR system.

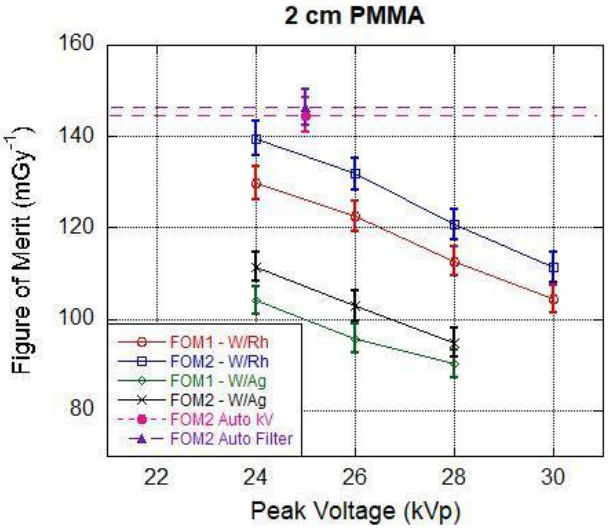

OPEN ACCESS
CC BY

Figure 6: Relation between FOM and Peak Voltage for 4 cm of PMMA in the analyzed DR system.

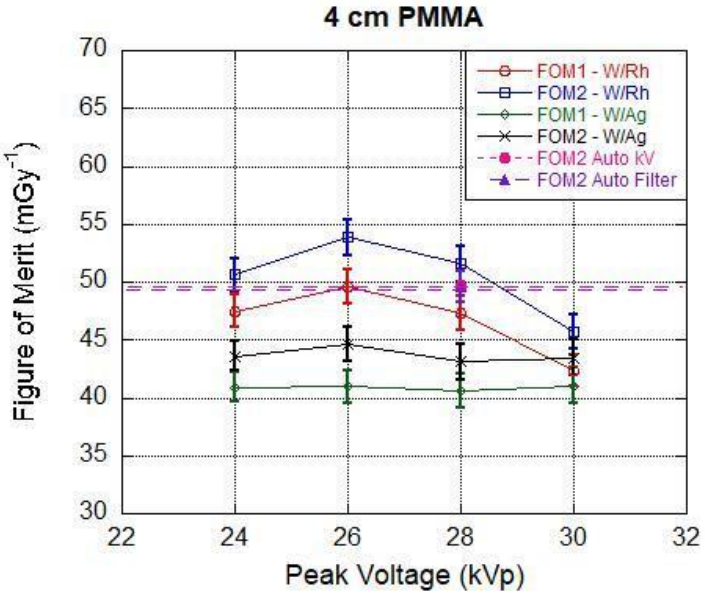

Figure 7: Relation between FOM and Peak Voltage for 7 cm of PMMA in the analyzed DR system.

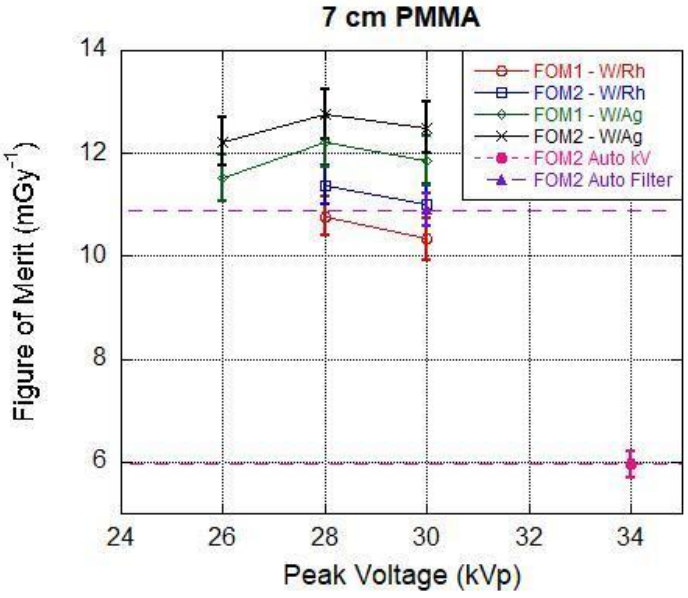

3.3 Analyzing the performance of the CR and the DR systems

In both analyzed systems, when a target-filter combination was fixed, the FOM curves presented similar tendencies. For the CR system, FOM1 was higher than FOM2, and the opposite was found for the DR system. Since the difference between the FOMs are

OPEN ACCESS

related to the calculation of CNR values, it is safe to affirm that the consideration of background's standard deviation affects directly the measure of image quality. Moreover, this standard deviation shows its bigger importance in DR systems, which can be related to image processing. The difference between FOM1 and FOM2 is found in the way to obtain the CNR, using Equations 2 and 3. The ratio between these relations is presented in Equation 5. CNR2 becomes CNR1 when the values for the standard deviations (σ_s and σ_{bg}) are the same. σ_s was higher than σ_{bg} for the CR system and lower for the DR system.

$$\frac{CNR1}{CNR2} = \frac{\sigma_s^2}{2\sigma_{bg}^2} + \frac{1}{2} \tag{5}$$

Together with the manual definition of the voltages and the target-filter combinations applied in the image acquisitions, the definition of the current-time product was made automatically by both analyzed CR and DR systems. The European Guidelines defines the standard deviation of a ROI as a measure of the noise in the output image [23]. The increase on the voltage and the consequent decrease on the mAs has caused variations in the standard deviations. For the CR system, the σ_s and σ_{bg} decreased with higher voltage values. On the other hand, for the DR system, the lower values for the deviations were related to lower values on the applied voltages.

4. CONCLUSIONS

The FOM was considered the parameter of optimization in the evaluation of the performance of a CR and a DR system. It was possible to verify that the FOM is related with exposure parameters, such as peak voltages, current time-product, breast thicknesses and target-filter combinations, a fact that is going towards what is given by the literature. Considering the same anode-filter combination for each thickness, FOM1 and FOM2 presented similar behavior, although FOM1 was higher than FOM2 for the CR system and

OPEN ACCESS

lower for the DR system. It can be explained by the influence of the standard deviation of the ROI positioned in the background.

Although both systems were studied, it is important to highlight the fact that it is not possible to compare the results directly, as the operation of the systems is significantly different. That is the reason why the analyses were made separately, each topic referring to each system.

The results obtained for the FOM are important in the discussion about the most suitable set of measurement parameters used for the image acquisitions. The optimization allows to find the balance between image quality and dose, making it possible to improve radiation protection and accurate diagnosis to the patient. Furthermore, the clinical routine in the studied institutions can be positively affected by the presented results, considering that the search for imaging parameters that provide results with diagnostic quality and lower dose involved is always fundamental, and the FOM can be considered to play an important role in this search.

ACKNOWLEDGMENT

The authors would like to thank the support and partnership provided by both of the Brazilian hospitals.

FUNDING

No funding was used in the development of this research.

CONFLICT OF INTEREST

All authors declare that they have no conflicts of interest.

OPEN ACCESS

CC BY

REFERENCES

[1] WCRF. World Cancer Research Fund International. Available at: https://www.wcrf.org/cancer-trends/worldwide-cancer-data/. Last access in: 06/27/2022.

[2] ACS. American Cancer Society. Available at: https://www.cancer.org/cancer/types/breast-cancer/about/how-common-is-breast-cancer.html. Last access in: 06/27/2022.

[3] INCA. Incidência. Rio de Janeiro, 2022. Disponível em: <https://www.gov.br/inca/pt-br/assuntos/gestor-e-profissional-de-saude/controle-do-cancer-de-mama/dados-e-numeros/incidencia>.

[4] OEFFINGER, K. C.; FONTHAM, E. T.; ETZIONI, R.; HERZIG, A.; MICHAELSON, J. S.; SHIH, Y. C. T.; WALTER, L. C.; CHURCH, T. R.; FLOWERS, C. R.; LAMONTE, S. J. Breast cancer screening for women at average risk: 2015 guideline update from the American Cancer Society. **Jama**, v. 314, n. 15, p. 1599-1614, 2015.

[5] GOLD, R. H.; BASSETT, L. W.; WIDOFF, B. E. Highlights from the history of mammography. **Radiographics**, v. 10, n. 6, p. 1111-1131, 1990.

[6] FREITAS, A. G.; KEMP, C.; LOUVEIRA, M. H.; FUJIWARA, S. M.; CAMPOS, L. F. Mamografia digital: perspectiva atual e aplicações futuras. **Radiologia Brasileira**, v. 39, p. 287-296, 2006.

[7] WOODARD, S.; MURRAY, A. Contrast-enhanced mammography: reviewing the past and looking to the future. In: Seminars in Roentgenology. WB Saunders, 2022, p. 126-133.

[8] XAVIER, A.; BARROS, V. S.; KHOURY, H. J.; MELLO, F. A. Avaliação da dose glandular média em sistemas digitais e convencionais de mamografia. In: International Joint Conference RADIO, Sociedade Brasileira de Proteção Radiológica. 2014.

[9] KANAGA, K.; YAP, H.; LAILA, S.; SULAIMAN, T.; ZAHARAH, M.; SHANTINI, A. A critical comparison of three full field digital mammography systems using figure of merit. **Med J Malaysia**, v. 65, n. 2, p. 119-122, 2010.

[10] MERAD, A.; SAADI, S.; KHELASSI-TOUTAOUI, N. Comparison of two full field digital mammography systems: Image quality and radiation dose. In: AIP Conference Proceedings. AIP Publishing LLC, v. 1994, n. 1, p. 060008, 2018.

OPEN ACCESS

[11] ACHO, S. N.; STOFILE, C.; MOLLER, M.; MORPHIS, M. Verification and optimisation of preselected exposure parameters in screening mammography: a central composite design methodology. **Radiation Protection Dosim**etry, v. 188, n. 3, p. 332-339, 2020.

[12] BUSHBERG, J. T.; BOONE, J. M. The essential physics of medical imaging. Lippincott Williams & Wilkins, 2011.

[13] NUNES, R.; BATISTA, W. Effect of target/filter combination on the mean glandular dose and contrast-detail threshold: A phantom study. **Radiography**, v. 27, n. 2, p. 272-278, 2021.

[14] NIROSHANI, H.; NAKAMURA, T.; MICHIRU, N.; NEGISHI, T. Influence of double layer filter on mean glandular dose (MGD) and image quality in low energy image of contrast enhanced spectral mammography (LE-CESM). **Radiography**, v. 28, n. 2, p. 340-347, 2022.

[15] AL KHALIFAH, K.; DAVIDSON, R.; ZHOU, A. Using aluminum for scatter control in mammography: preliminary work using measurements of CNR and FOM. **Radiological Physics and Technology**, v. 13, p. 37-44, 2020.

[16] SHARMA, R.; SHARMA, S.; SARKAR, P.; DATTA, D. Imaging and dosimetric study on direct flat-panel detector-based digital mammography system. **Journal of Medical Physics**, v. 43, n. 4, p. 255, 2018.

[17] BORG, M.; BADR, I.; ROYLE, G. The use of a figure-of-merit (FOM) for optimisation in digital mammography: a literature review. **Radiation Protection Dosimetry**, v. 151, n. 1, p. 81-88, 2012.

[18] BORG, M.; KONSTANTINIDIS, A. Alternative figures-of-merit in digital mammography. **Radiation Protection Dosimetry**, v. 176, n. 4, p. 388-399, 2017.

[19] BALDELLI, P.; PHELAN, N.; EGAN, G. Investigation of the effect of anode/filter materials on the dose and image quality of a digital mammography system based on an amorphous selenium flat panel detector. **The British journal of radiology**, v. 83, n. 988, p. 290-295, 2010.

[20] MORAIS, I. S.; SQUAIR, P. L.; TAVARES, M. S. N. Optimization of exposure parameters in digital mammography (CR) using figure of merit. **Brazilian Journal of Radiation Sciences**, v. 9, n. 1A, 2021.

OPEN ACCESS

CC BY

[21] FAUSTO, A. M.; LOPES, M.; SOUSA, M.; FURQUIM, T. A.; MOL, A. W.; VELASCO, F. G. Optimization of image quality and dose in digital mammography. **Journal of digital imaging**, v. 30, p. 185–196, 2017.

[22] PEREZ, A. M.; POLETTI, M. E.; TOMAL, A.; CORREIA, P. D.; PACIÊNCIA, R. D.; SILVA, M. C. Study of optimization in CR and DR digital mammography systems. **Revista Brasileira de Física Médica**, v. 11, n. 2, p. 11-15, 2017.

[23] PERRY, N.; BROEDERS, M.; DE WOLF, C.; TÖRNBERG, S.; HOLLAND, R.; VON KARSA, L. European guidelines for quality assurance in breast cancer screening and diagnosis. - summary document. Oncology in Clinical Practice, v. 4, n. 2, p. 74-86, 2008.

[24] IAEA. International Atomic Energy Agency. Dosimetry in diagnostic radiology: an international code of practice. 2007.

[25] PROTECTION, Radiological. ICRP Publication 103. Ann ICRP, v. 37, n. 2.4, p. 2, 2007.

[26] BRASIL. Resolução CNEN no 164/14. Norma CNEN NN-3.01 Diretrizes Básicas de Proteção Radiológica. Diário Oficial da República Federativa do Brasil, Ministério da Ciência e Tecnologia, Brasília, DF, 2005.

[27] DANCE, D.; SKINNER, C.; YOUNG, K.; BECKETT, J.; KOTRE, C. Additional factors for the estimation of mean glandular breast dose using the UK mammography dosimetry protocol. **Physics in medicine & biology**, v. 45, n. 11, p. 3225, 2000.

[28] SCHNEIDER, C. A.; RASBAND, W. S.; ELICEIRI, K. W. NIH image to ImageJ: 25 years of image analysis. **Nature methods**, v. 9, n. 7, p. 671–675, 2012.

[29] LAZZARO, M. V.; LUZ, R. M.; CAPAVERDE, A. S.; SILVA, A. M. M. Avaliação comparativa da qualidade da imagem em sistemas de radiologia computadorizada utilizando Imaging Plates com diferentes tempos de uso. **Revista Brasileira de Física Médica (Online)**, 2015.

[30] SILVA, R. H. B. S. Estudo de otimização de sistemas mamográficos utilizando FOM (Figura de Mérito). 2017.

[31] IAEA. International Atomic Energy Agency. Quality assurance programme for digital mammography. 2011.

OPEN ACCESS

CC BY

[32] BRASIL. Instrução Normativa - IN n° 92, de 27 de maio de 2021. Diário Oficial da União, Ministério da Saúde, Agência Nacional de Vigilância Sanitária, Diretoria Colegiada, 2021.

[33] OLIVEIRA, B. B.; OLIVEIRA, M. A.; PAIXÃO, L.; TEIXEIRA, M. H. A.; NOGUEIRA, M. S. Dosimetria e avaliação da qualidade da imagem em um sistema de radiografia direta. **Radiologia Brasileira**, v. 47, p. 361–367, 2014.

[34] JAKUBIAK, R.; GAMBA, H.; NEVES, E.; PEIXOTO, J. Image quality, threshold contrast and mean glandular dose in CR mammography. **Physics in Medicine & Biology**, v. 58, n. 18, p. 6565, 2013.

LICENSE

This article is licensed under a Creative Commons Attribution 4.0 International License, which permits use, sharing, adaptation, distribution and reproduction in any medium or format, as long as you give appropriate credit to the original author(s) and the source, provide a link to the Creative Commons license, and indicate if changes were made. The images or other third-party material in this article are included in the article's Creative Commons license, unless indicated otherwise in a credit line to the material.
To view a copy of this license, visit http://creativecommons.org/ licenses/by/4.0/.